

Cite this: *Sustainable Food Technol.*,  
2026, 4, 1953

# Transparent and water-resistant edible coatings for sustainable post-harvest preservation of banana

Yilun Weng,<sup>\*a</sup> Yan Zhu,<sup>a</sup> Yue Ren,<sup>a</sup> Hale Oguzlu,<sup>b</sup> Heather Shewan <sup>b</sup>  
and Alberto Baldelli <sup>\*ac</sup>

The rapid spoilage of fresh produce due to water loss remains a major challenge in the post-harvest preservation of fruits and vegetables. While current solutions often rely on plastic packaging, these approaches pose environmental concerns and offer limited biodegradability. This study presents a sustainable alternative by developing transparent and water-resistant edible coatings using a spray-coating method based on natural materials, including gelatin (GE), gum arabic (GA), milk protein isolate (MPI), and coconut oil (CO). Spray coatings were prepared using two groups of formulations, including the GE-based group and the GA-based group. Their physicochemical and functional properties, including visual appearance, hydrophobicity, film thickness, surface roughness, and morphology were systematically evaluated. The optimal formulations identified were 4% GE, 2% MPI, and 4% CO (sample 1-424) for the GE-based group, and 5% GA, 4% MPI, and 1% CO (sample 2-541) for the GA-based group. Both coatings exhibited relatively smooth surfaces, high transparency, and strong water resistance. When applied to bananas stored at room temperature for 10 days, these coatings significantly reduced water loss and delayed visible signs of ripening. These findings highlight the potential of the developed spray coatings for post-harvest preservation. Overall, this work introduces a novel edible coating system that combines food preservation efficacy with environmental sustainability, offering promising applications in green packaging and the large-scale post-harvest treatment of fresh produce.

Received 31st October 2025  
Accepted 17th December 2025

DOI: 10.1039/d5fb00804b

rsc.li/susfoodtech

## Sustainability spotlight

This work demonstrates a sustainable alternative to plastic packaging through the development of transparent, water-resistant, edible coatings for bananas using gelatin, gum arabic, milk proteins, and natural lipids. By reducing fruit weight loss by ~40%, extending shelf-life by up to five days, and maintaining high transparency (>90%), the coatings enable effective preservation without reliance on synthetic polymers. This aligns with the UN Sustainable Development Goals (SDGs), particularly SDG 12: Responsible Consumption and Production and SDG 13: Climate Action, by reducing food waste and mitigating plastic pollution. Our findings highlight how natural, biodegradable materials can be applied at scale in fresh produce supply chains, advancing both food security and environmental sustainability.

## 1 Introduction

The postharvest physiological activity of fresh produce substantially limits its shelf life. Continuous respiration and enzymatic reactions accelerate biochemical deterioration, including enzymatic browning (color loss), oxidative stress (nutrient degradation), and transpiration (water loss).<sup>1</sup> For example, lettuce remains acceptable for up to 7 days under refrigeration but deteriorates within 1–2 days at ambient conditions; strawberries, blueberries, and cherries typically last 5–9 days when refrigerated but only 2–3 days without cooling;

and pears, although more robust, decline from 2–3 weeks in cold storage to just a few days at room temperature.<sup>2</sup> These sharp reductions underscore the urgent need for effective preservation strategies, particularly in warm and humid regions where cold chain infrastructure remains inadequate. To counteract such rapid deterioration, diverse packaging technologies have been developed to prolong shelf life and maintain freshness, though each comes with technical and environmental limitations.

Modern packaging technologies play a pivotal role in extending shelf life and maintaining the quality of fresh produce. Conventional methods focus on controlling environmental parameters: refrigeration slows down metabolic activity through temperature control, vacuum packaging inhibits microbial growth by removing oxygen, and modified atmosphere packaging (MAP) dynamically adjusts gas composition to delay ripening and spoilage.<sup>3</sup> However, high-moisture

<sup>a</sup>School of Agriculture and Food Sustainability, The University of Queensland, Australia. E-mail: a.baldelli@uq.edu.au

<sup>b</sup>School of Chemical Engineering, The University of Queensland, Australia

<sup>c</sup>The Queensland Alliance for Agriculture and Food Innovation (QAAFI), The University of Queensland, Australia



produce such as berries still presents major challenges, as existing methods often fail to effectively prevent cellular degradation and moisture loss.<sup>4</sup> These limitations highlight the technical bottleneck in current packaging solutions. Additionally, most conventional packaging relies heavily on petroleum-based plastics. While plastics offer advantages such as low cost, durability, and formability, they present significant environmental and health risks.<sup>5</sup> These materials degrade extremely slowly, with mineralization cycles lasting hundreds of years, leading to accumulation in landfills and aquatic environments. Globally, over 300 million tons of plastic waste are generated annually, yet less than 10% is recycled.<sup>6</sup> Among the more than 900 chemical compounds used in plastic packaging, many are known to be persistent, bioaccumulative, toxic, or endocrine-disrupting.<sup>7</sup> Thus, there is a growing demand for sustainable packaging alternatives that align with environmental safety and food-grade requirements.

In response, recent research has shifted toward functional interface modification technologies, particularly the development of protective edible coatings with great water resistance and optical transparency. These two properties are critical for food applications: hydrophobicity helps reduce moisture loss and respiration, while transparency ensures that the natural appearance of the fruit or vegetable is preserved for consumer appeal. However, most current edible coatings face limitations such as plasticizer migration, high cost per unit area, limited transparency, and poor mechanical durability under stress (*e.g.*, cracking after bending).<sup>8–10</sup> Additionally, the scalability of the spray-coating process is a critical consideration for translating laboratory-scale findings into industrial practice. Optimizing key parameters such as coating formulation, spray uniformity, and drying conditions is essential to ensure consistent film performance during large-scale operations.<sup>11</sup> Addressing these aspects will enhance the feasibility of adopting biopolymer-based coatings as sustainable alternatives to conventional plastic packaging in food preservation.

To address these challenges, this study proposes a novel edible spray coating system formulated with food-grade, bio-based materials. Using natural biopolymers, including GA, GE, and MPI, as well as CO, the coating was engineered to enhance gas barrier properties, improve hydrophobicity, and maintain transparency. Overall, this study introduces an innovative and scalable edible coating system that offers a promising strategy for post-harvest preservation while contributing to environmental sustainability. First, the optimal operational conditions of spraying such as spraying angle, duration, and distance were investigated and optimized. Secondly, a range of GA- and GE-based formulations were developed, and the properties of both feed solutions and the dried films were analyzed, including microstructure, film thickness, surface morphology and roughness, color, contact angle, and light transmittance. In the end, the effect of this coating on banana preservation for up to 10 days was evaluated. The coating effectively reduced water loss and delayed visible ripening symptoms such as browning and softening. By integrating material innovation with the spray coating technology, this study provides a practical solution to extend the shelf life of fresh produce and reduce dependency on plastic-based packaging.

## 2 Materials and methods

### 2.1 Materials

GA from acacia tree was purchased from Sigma-Aldrich (CAS-No.: 9000-01-5). MPI was supplied by Ingredia (Arras, France), which contains 85% protein based on dry matter content. CO from *Cocos nucifera* was purchased from Sigma-Aldrich (low-melting solid coconut oil, CAS-No.: 8001-31-8). GE was kindly provided by Gelita (Edible Beef Skin (Type B) Gelatin Powder, Beaudesert, Australia). All other chemicals used in this work were purchased from Sigma-Aldrich and were used as received. Milli-Q water (MQW) with a minimum resistivity of 18.2 MΩ cm (Millipore, Australia) was used for all experiments.

### 2.2 Preparation of the spray coating solution

Based on the pre-experiments and the literature, 14 formulations of GA-based group (group 1) and GE-based group (group 2) were prepared (Table 1). Samples were denoted as (their group name) – (the concentration of each of the components). For example, sample 1-642 has a formulation matrix of 6% GA, 4% MPI, and 2% CO. Briefly, GA/GE and MPI were weighed and dispersed in 100 mL of water, with magnetic stirring for 60 minutes at 40 °C, to completely dissolve GA and GE. Subsequently, the solution was heated at 80 °C for 30 minutes to denature the MPI. After heating, a certain amount of CO was added. The spray feed solutions (pH = 6–7) were sufficiently mixed to form stable emulsions using a Turrax homogenizer (IKA, Germany) at 10 000 rpm for 3 min at room temperature. Finally, the viscosity and transmittance of the solution were recorded prior to spraying.

### 2.3 Preparation of the spray coating

The as-prepared spray coating solutions were sprayed onto pre-cleaned and dried flat glass surfaces (Menzel-Glaser microscope slides, approximately 76 × 26 mm, Australia) using a battery-powered spray gun (18 V, PXOSGS-018, Ozito, Australia) with a nozzle diameter of 1.3 mm. Three different spray distances,

**Table 1** A formulation matrix of edible coating solutions with different proportions of GA, GE, MPI, and CO (g per 100 mL)

Sample name	GA	GE	MPI	CO
1-642	6	0	4	2
1-541	5	0	4	1
1-532	5	0	3	2
1-442	4	0	4	2
1-424	4	0	2	4
1-324	3	0	2	4
1-342	3	0	4	2
1-243	2	0	4	3
2-422	0	4	2	2
2-424	0	4	2	4
2-442	0	4	4	2
2-444	0	4	4	4
2-522	0	5	2	2
2-224	0	2	2	4



including 5 cm, 10 cm, and 15 cm, and various spraying angles and durations were tested as pre-experiments. The optimized spraying conditions were obtained from pre-experiments prior to spraying these developed formulations. The sprayed glass plates were then placed in a well-ventilated area at room temperature and left to dry for 24 hours, allowing complete solvent (water) evaporation.

## 2.4 Characterization of the spray coating

**2.4.1 Color profile analysis.** The surface color parameters of the film samples were measured using a spectrophotometer operating in the Commission on Illumination (CIE) Lab color space, which precisely quantifies visual color attributes.<sup>12</sup> For each film sample, measurements were taken from three distinct, randomly selected regions. The recorded color parameters included  $L^*$ , representing the degree of lightness;  $a^*$ , indicating the red-green chromaticity axis; and  $b^*$ , denoting the yellow-blue chromaticity axis. Subsequently, the collected values were calculated as averages and reported as mean  $\pm$  standard deviation.

A standard plate, specifically a clear glass slide without film coating, served as the baseline reference for the color measurements. The measured reference values were  $L^* = 92.2$ ,  $a^* = -0.62$ , and  $b^* = 3.7$ . These baseline readings facilitated the calculation of color deviations for the film samples relative to a neutral and consistent reference point.

The total color difference ( $\Delta E$ ) was calculated using the following equation:

$$\Delta E = \sqrt{(\Delta L)^2 + (\Delta a)^2 + (\Delta b)^2}$$

where  $\Delta L$ ,  $\Delta a$ , and  $\Delta b$  represent the specific differences in the measured lightness and chromatic coordinates between the film samples and the standard reference. A higher  $\Delta E$  value indicates greater perceptible differences in color compared to the reference.

**2.4.2 Static contact angle measurement.** The hydrophobicity of the film was evaluated by measuring the water contact angle at room temperature (25 °C). A contact angle goniometer (OCA 15EC, DataPhysics Instruments GmbH, Germany) was used for this purpose. To ensure accurate results, each film was measured at three randomly chosen spots. The average of these three values was used to represent the film's overall wettability.

**2.4.3 Film surface structure, thickness, and roughness analysis.** The surface structure of the films was examined with a digital microscope (DFC450C, Leica Microsystems Ltd, Germany). Zeta 300 Optical Profilometer (CN Tech, UK) was used to measure the surface roughness and thickness of the coatings. The investigated area was first nominated optically using the system's live imaging feature under different objective magnifications (e.g., 10 $\times$ , 20 $\times$ , or 50 $\times$ ) to ensure accurate selection without any physical contact. The profilometer operates in non-contact mode, which prevents any surface damage. After identifying the target area, a 3D scan was performed to obtain detailed surface topology and roughness parameters such as  $S_a$  and  $S_q$ . Arithmetic mean roughness ( $S_a$ ) and root mean square

roughness ( $S_q$ ) were calculated from 3D optical profilometry data using the built-in analysis software ( Alicona IF-M, Austria).

**2.4.4 Effect of coatings on banana preservation.** Bananas with consistent maturity and no damage to the skin were purchased from Coles Supermarket (Brisbane, Australia) and randomly divided into the control group (unsprayed) and the experimental group (sprayed with 1-541 for the GA-based group and with 2-424 for the GE-based group). Bananas were stored in an environment with a temperature of 20 °C and a humidity of 60%. The weight loss of bananas was recorded daily, and the weight loss rate was calculated based on the equation:

$$\text{Weight loss rate} = (W_0 - W_t)/W_0 \times 100\%$$

where  $W_0$  is the initial weight of the banana and  $W_t$  is the weight of the banana after certain storage periods. A sensory analysis, which includes a visual analysis of changes in color and texture, and olfactory analysis of changes in aroma, was conducted by three independent assessors.

## 2.5 Statistical analysis

Experiments were repeated at least three times independently. Statistical analysis was conducted using a t-test and one-way analysis of variance (ANOVA) was employed for multiple comparisons (GraphPad Prism 10). Levels of statistical significance are \* $p < 0.05$ , \*\* $p < 0.01$ , \*\*\* $p < 0.001$ .

## 3 Results and discussion

Before conducting spray coating experiments with the designed formulations (Table 1), a preliminary study was performed to optimize spray distance, angle, and duration (Fig. S1). Spray distance influences particle flight time, impacting their temperature and velocity upon substrate impact, and thus the coating formation process.<sup>13</sup> The optimal conditions were set to a 15 cm distance, 45° angle, and 10 s duration. Feed solutions were then characterized based on viscosity and light transmittance (Table S1 and Fig. S3). Viscosity governs fluidity, spreadability, film thickness, adhesion during spraying, and structural integrity after drying, which in turn affect coating uniformity, curing behavior, and barrier properties.<sup>14</sup> Most of the feed solutions showed a viscosity below 10 mPa s (Fig. S2 and Table S1), making it easy to spray without nozzle clogging. Light transmittance, critical for visually transparent food packaging, reflects coating compactness, uniformity, and phase distribution. The results indicated that the feed solutions were not as transparent, as all formulations showed a transmittance below 30% (Fig. S3). However, this transmittance alone does not fully reflect the transparency of the coating. Physical processing parameters and structural properties of the coating also play a critical role in determining final light transmission. Furthermore, the images of the spray coating on transparent glass slides (Fig. S1, S2 and S4) showed the relative transparency of the coatings. Subsequent sections detail the dried film's visual appearance, physical and microstructural properties, and fruit preservation performance.



### 3.1 Microstructure observation, coating thickness, and roughness

The microstructure of edible coatings plays a crucial role in determining their physical stability, barrier properties and adhesion to the substrate. The microscope images of films were taken (Fig. 1) and their surface morphology and microstructure characteristics of all sample formulations were systematically analyzed. The key points of analysis include surface integrity as well as uniformity of particle distribution. These structural characteristics directly affect the film-forming quality and barrier function of the coating.

Among GA-based group, sample 1-541 showed the most desirable characteristics, with continuous and smooth surface, and uniform particle distribution, followed by sample 1-442. In addition, the CO added to the formula may also play a role, helping to improve structural uniformity and strengthen the plasticizing network within the film. The performance advantages of 1-541 may be attributed to the optimized configuration of the materials ratio, which enables better compatibility and less phase separation among biopolymers. In contrast, samples 1-243 and 1-642 showed clear signs of inhomogeneity and particle aggregation. Localized regions contain noticeable disrupted film continuity, which are likely to impair vapor barrier efficiency and adhesion properties.

Among GE-based group, samples with a higher MPI content, such as 2-422 and 2-522 typically showed denser and more continuous matrix networks, with smaller and more uniformly distributed oil droplet voids. In contrast, formulations with higher GE content or an MPI/GE ratio of 1 : 1 (e.g., 2-224, 2-424, and 2-444) displayed looser structures, with larger pores or irregular cavities and localized matrix discontinuity. Overall, as the MPI ratio decreased or oil content increased, the continuity and uniformity of the microcapsule wall matrix declined significantly. The comparative observation results of each formula in terms of microstructure were summarized in Table S3.

The microscopic observations assessed the surface uniformity and structural integrity of each edible coating formulation. The surface microstructure provides insight into film integrity, as uniform and crack-free morphology often indicates cohesive structure and reduced susceptibility to moisture or gas diffusion. To further quantify the film properties, five formulations from each group were chosen for 3D surface profilometry. These samples exhibited relatively continuous surfaces without severe damage or obvious bubble defects. The thickness and roughness parameters, including average thickness, arithmetic mean roughness ( $S_a$ ), and root mean square roughness ( $S_q$ ) were obtained to systematically evaluate the film quality.  $S_a$  represents the average height deviation of the surface profile from the mean plane, providing an overall measure of the general

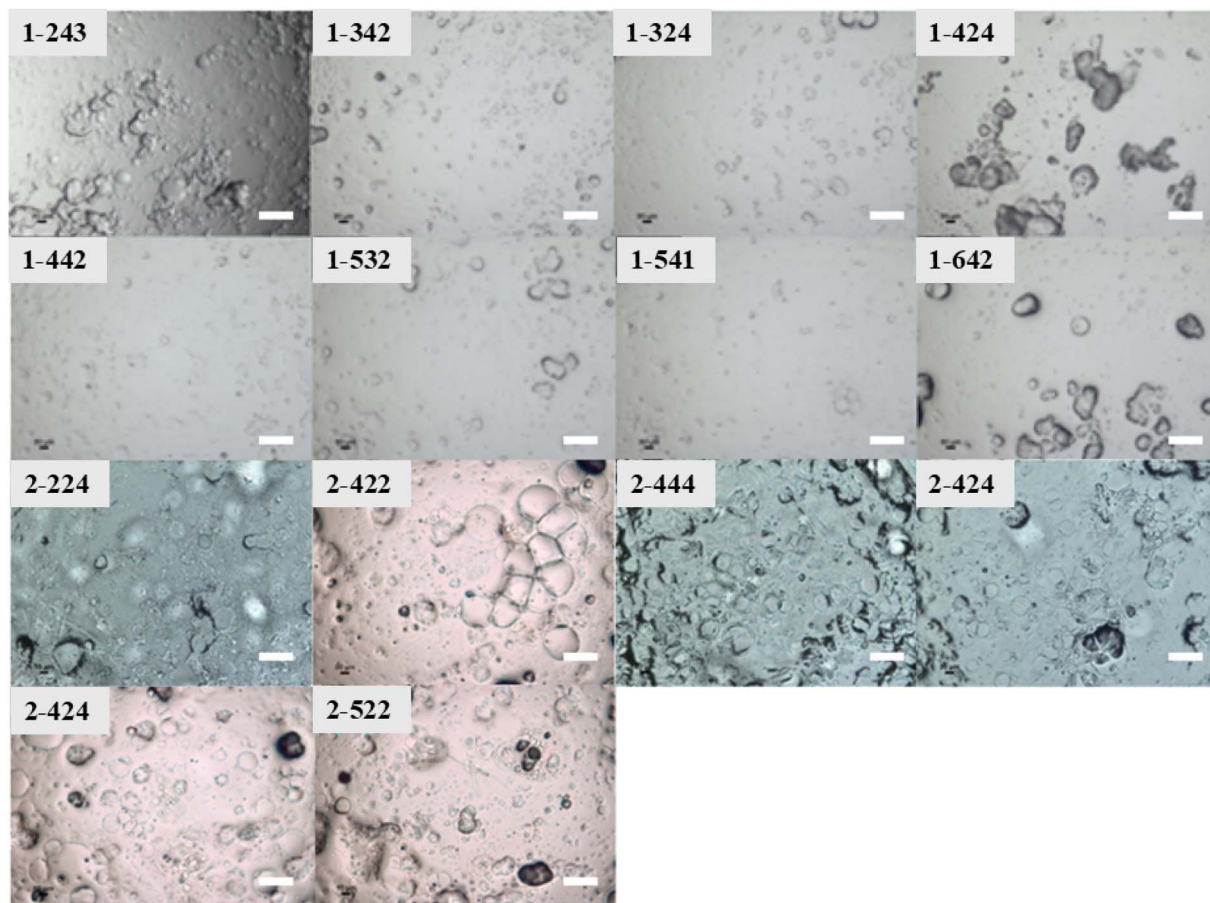


Fig. 1 Microscope images of coatings. Scale bars = 100  $\mu$ m.



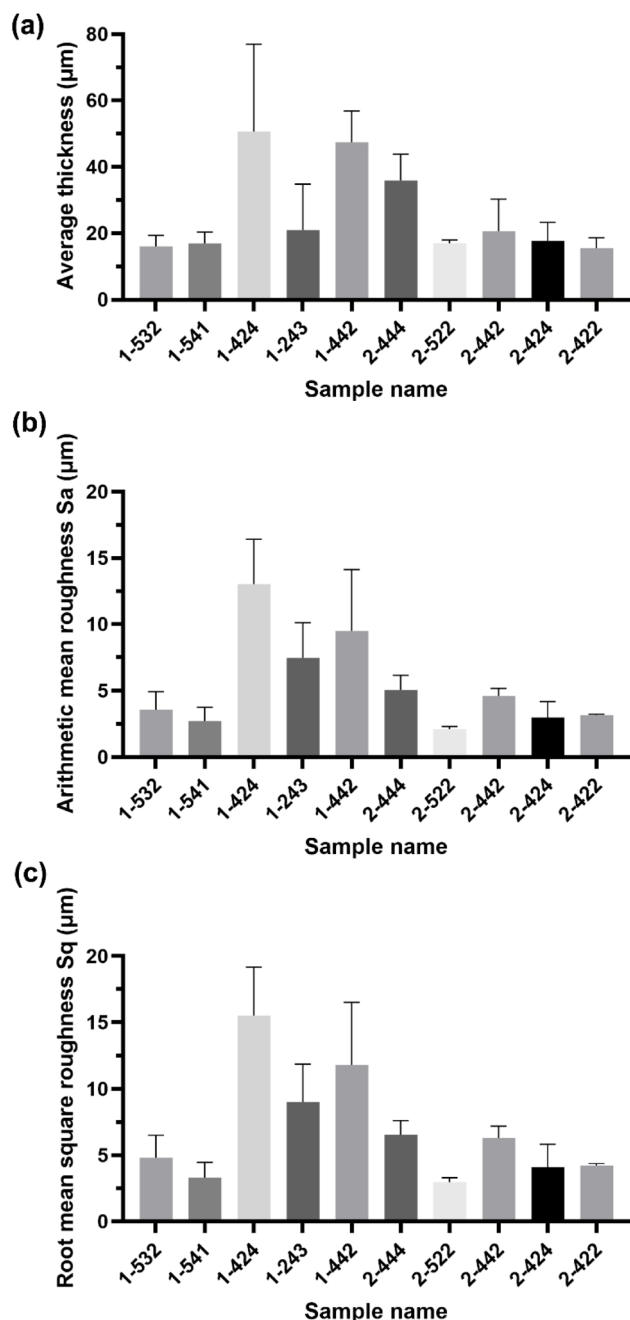


Fig. 2 Surface thickness (a), arithmetic mean roughness (b), and root mean square roughness (c) of spray coatings.

roughness level without disproportionately weighting larger deviations. In contrast,  $S_q$  is calculated as the square root of the mean of the squared height deviations, making it more sensitive to pronounced surface irregularities such as high peaks or deep valleys. Consequently, a noticeably higher  $S_q$  compared to  $S_a$  indicates the presence of significant topographical features on the coating surface.

Most of the samples measured showed a thickness around 20  $\mu\text{m}$ , except for samples 1-424 and 1-442 which were over 40  $\mu\text{m}$  in thickness. The GA-based group exhibited greater thickness than the GE-based group. Samples 1-424 and 1-243 had the highest standard deviation (SD) among all samples (Fig. 2a),

indicating the most non-uniform surface, which is in line with the microscope images (Fig. 1) and the 3D images (Table 2).

Among GA-based group, sample 1-541 demonstrated the lowest surface roughness ( $S_a = 2.71 \mu\text{m}$ ,  $S_q = 3.29 \mu\text{m}$ ). This lower surface roughness not only represents a more uniform film surface morphology but may also exhibit better stability in tribological properties. According to Doruker and Mattice, an increase in surface roughness will broaden the interfacial density distribution of the film and reduce the diffusion ability of polymer chains in the film surface direction, thereby weakening its structural integrity.<sup>15</sup> The smoother surfaces of sample 1-541 facilitate the ordered arrangement of molecular chains and the enhancement of interfacial bonding, thereby improving their film performance. Lower surface roughness not only leads to a more uniform surface morphology but also helps to reduce light scattering and optical distortion. According to the findings of Larena *et al.*, it showed that in a multilayer polymer system, an increase in  $S_a$  significantly reduced the light transmittance and interferes with the clarity of the interference fringes.<sup>16</sup> Therefore, the smoother surface morphology exhibited by sample 1-541 not only benefits the improvement of visual appearance but also helps to achieve better functional optical performance.

For GE-based groups, the oil content deeply influenced film continuity and roughness. When lipid content is insufficient, the film structure can exhibit fragmentation.<sup>17</sup> For example, in sample 2-442, the proportion of CO was half that of 2-444, which approximately halved the surface thickness and decreased  $S_a$  (Fig. 2). During drying and film formation, the small amount of lipid tends to migrate upwards and aggregate, failing to form a continuous lipid layer. Studies suggest that highly hydrophobic components migrating upwards and partially volatilizing or precipitating during drying can leave porous, cavity-like structures, creating discontinuities within the film layer.<sup>17</sup> Although CO does not volatilize, the limited oil phase in sample 2-442 may aggregate into isolated patches, resulting in localized areas lacking lipid filling and thus forming discontinuous depressions or voids. This can explain the discontinuities observed in the 3D surface morphology of sample 2-442. Moreover, due to lower lipid content, the lack of sufficient hydrophobic filling between protein networks may cause concentrated stress during drying shrinkage, exacerbating microcracking and further increasing roughness. Conversely, higher lipid content helps form a more complete lipid surface layer, reducing overall roughness, provided the emulsion system is sufficiently stable to prevent large-scale oil phase separation.<sup>18</sup> For samples 2-444 and 2-424, for instance, the higher lipid content, coupled with ample MPI, resulted in finely dispersed oil droplets and a homogeneous single-layer structure, consistent with literature reports that uniform dispersion of the hydrophobic phase within a matrix (single-layer films) can maintain structural continuity.

In summary, the ratio of proteins to lipids determines the microscopic surface characteristics of edible films by influencing emulsification, dispersion, and phase separation behaviors. When GA : MPI or GE : MPI proportions are balanced and emulsification is sufficient (such as sample 2-444), the lipids embed uniformly within the protein matrix as small



Table 2 Surface characteristics of coatings, including 3D surface morphology, surface thickness, and roughness

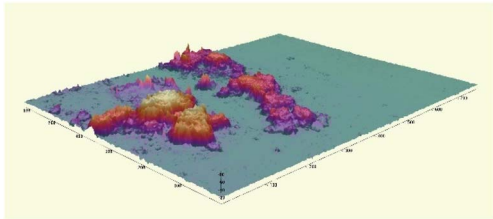
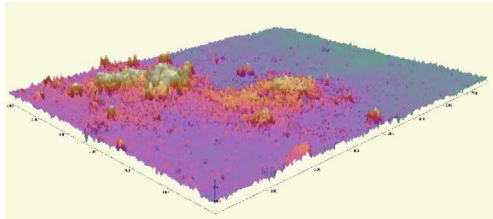
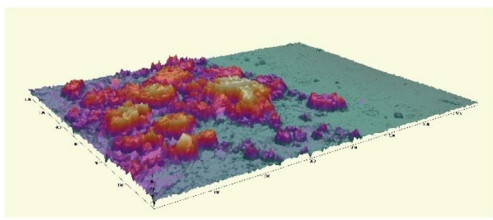
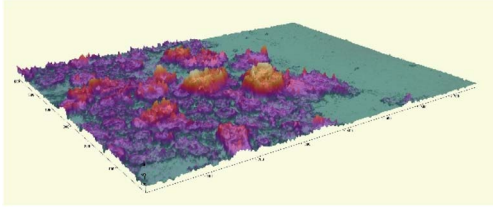
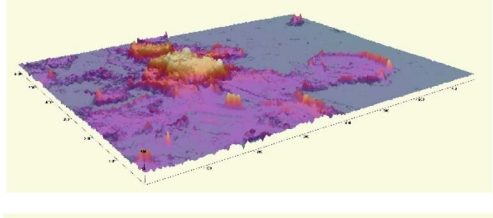
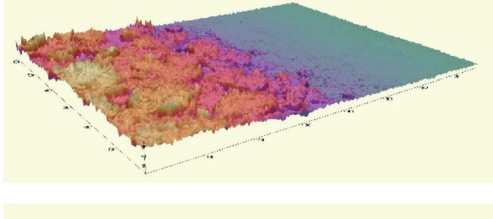
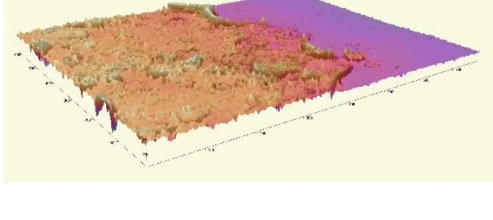
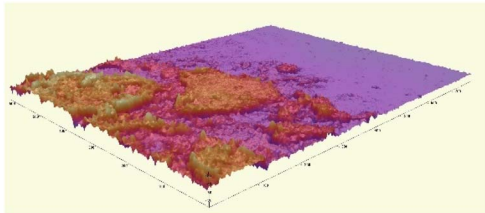
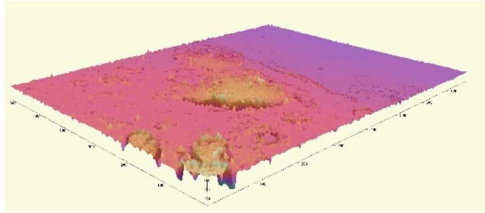
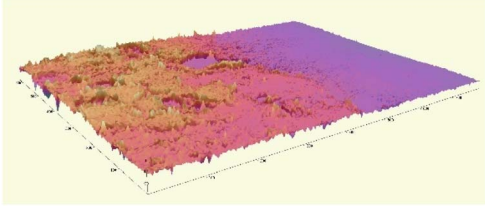
Sample name	3D image	Average thickness ( $\mu\text{m}$ )	$S_a$ ( $\mu\text{m}$ )	$S_q$ ( $\mu\text{m}$ )
1-532		$15.95 \pm 3.37$	$3.55 \pm 1.38$	$4.81 \pm 1.7$
1-541		$16.81 \pm 3.47$	$2.71 \pm 1.03$	$3.29 \pm 1.16$
1-424		$50.61 \pm 26.34$	$13.02 \pm 3.39$	$15.51 \pm 3.66$
1-243		$20.89 \pm 13.94$	$7.46 \pm 2.65$	$9.02 \pm 2.86$
1-442		$47.40 \pm 12.20$	$9.47 \pm 4.65$	$11.80 \pm 4.70$
2-444		$35.87 \pm 7.96$	$5.05 \pm 1.11$	$6.55 \pm 1.06$
2-522		$16.94 \pm 0.99$	$2.11 \pm 0.19$	$2.98 \pm 0.33$



Table 2 (Contd.)

Sample name	3D image	Average thickness ( $\mu\text{m}$ )	$S_a$ ( $\mu\text{m}$ )	$S_q$ ( $\mu\text{m}$ )
2-442		$20.58 \pm 9.66$	$4.60 \pm 0.57$	$6.30 \pm 0.89$
2-424		$17.60 \pm 5.65$	$2.98 \pm 1.19$	$4.10 \pm 1.72$
2-422		$15.43 \pm 6.73$	$3.16 \pm 0.07$	$4.22 \pm 0.16$

droplets, leading to a continuous and relatively smooth film surface. However, when MPI is insufficient or protein proportions are imbalanced (such as sample 2-424), lipids tend to aggregate into layers, significantly increasing surface roughness and resulting in noticeable layering irregularities. With excessively low lipid content (such as sample 2-442), the inherent protein-protein aggregation becomes apparent due to insufficient lipid filling, manifesting as localized film fragmentation, discontinuities, and increased roughness.<sup>18</sup> These observations align with the protein-lipid synergy mechanisms described in related literature: proteins provide the matrix backbone and emulsifying interfaces, while adequate emulsifier (*e.g.*, MPI) stabilizes the oil phase and maintains homogeneous structure. Protein compatibility and balanced ratios directly affect network density and integrity. The significant variations in surface roughness ( $S_a$ ,  $S_q$ ) and height differences observed among different formulations clearly reflect these microscale structural changes. Consequently, optimizing protein-to-lipid ratios to control interactions and phase separation is crucial for preparing edible packaging films with smooth surfaces and continuous structures.

### 3.2 Color analysis

The color of food plays a crucial role in shaping consumers' first impression and acceptance. Even the slightest change in color can affect its sensory evaluation and market appeal. Therefore, the stability and uniformity of color are important indicators for

evaluating the appearance and functional performance of edible coatings. In edible coatings, the surface color is not only influenced by the composition of the formula but also reflects a combination of factors such as molecular interactions and film formation uniformity.<sup>19</sup>

Through the quantitative analysis of color difference parameters such as  $L^*$ ,  $a^*$ ,  $b^*$  and  $\Delta E$ , an evaluation basis can be provided for the transparency and color of the coating. The  $L$ -value indicates brightness, extending from a value of 0, which represents black, to a maximum of 100, which represents white. The  $a^*$  value represents the red-green axis, indicating that positive values correspond to red, while negative values correspond to green. Similarly, the  $b^*$  value pertains to the yellow-blue axis, where positive values indicate yellow and negative values indicate blue. The  $\Delta E$  value is used to measure the total difference from a certain standard or initial color. The higher the  $\Delta E$  value, the more obvious the color changes. In particular, the  $\Delta E$  value, as a sensitive parameter for measuring the deviation of the coating color from the standard reference (uncoated slides), is of great significance for judging whether the color is acceptable. To explore the influence of different GA/GE/MPI/CO ratios on the color properties of the coating, a variety of formulations were prepared in this study and detected by a colorimeter. The results are summarized in Table 3, after subtracting the  $L$ ,  $a$ , and  $b$  values of an uncoated glass substrate ( $L_0^* = 92.2$ ,  $a_0^* = -0.62$ ,  $b_0^* = 3.7$ ).



**Table 3** Colorimetric properties ( $\Delta L$ ,  $\Delta a$ ,  $\Delta b^*$ , and  $\Delta E$ ) of coatings prepared from various formulations

Sample name	$\Delta L^*$	$\Delta a^*$	$\Delta b^*$	$\Delta E$
1-642	-3.97	-0.13	0.99	4.09 ± 0.16
1-541	-1.38	-0.01	0.15	1.38 ± 0.05
1-532	-3.66	-0.1	0.35	3.68 ± 0.07
1-442	-1.53	0	0.03	1.53 ± 0.03
1-424	-3.86	-0.1	0.7	3.92 ± 0.11
1-324	-4.29	-0.09	0.73	4.36 ± 0.09
1-342	-4.02	-0.14	0.51	4.05 ± 0.13
1-243	-3.13	-0.03	0.23	3.14 ± 0.09
2-422	-2.13	-0.05	0.10	1.59 ± 0.07
2-424	-1.41	-0.04	0.26	1.52 ± 0.07
2-442	-2.53	-0.04	0.34	2.79 ± 0.08
2-522	-1.41	-0.04	0.26	1.52 ± 0.06
2-444	-1.66	-0.04	0.06	1.78 ± 0.04
2-224	-1.44	-0.01	-0.03	1.44 ± 0.05

Overall, all coatings showed a decreased brightness (negative  $\Delta L^*$ ) compared to uncoated glass, as well as a negative  $\Delta a^*$ , indicating that all films slightly shifted toward the green axis, probably attributed to the presence of polysaccharides and the MPIs (Table 3). The  $\Delta b^*$  values showed that most films had a yellowish shift, except for sample 2-224, which exhibited a negative value, indicating a slight blue hue, probably attributed to the high CO content in the formulations.

For the GA-based group, the results of color difference analysis showed that the average luminance ( $L^*$ ) of all coated samples is relatively high, ranging from 87.91 to 90.83. Sample 1-541 had the highest brightness, while sample 1-324 was slightly darker. The negative  $a^*$  value indicated that the samples generally have a slight greenish tint with a small variation range. The charge neutralization effect between MPI and GA may selectively absorb the red-light band and enhance green light reflection.<sup>20</sup> The  $b^*$  values were all positive, ranging from 3.73 to 4.69, showing a light-yellow characteristic. Among them, sample 1-642 had the strongest yellow bias. High oil content ( $\geq 2\%$ ) may accelerate lipid oxidation and generate yellow peroxides.<sup>21</sup> The slight yellow may be attributed to the native color of GA and the presence of residual sugars and proteins that may undergo mild Maillard reaction or caramelization during drying.<sup>22</sup> The color difference ( $\Delta E$ ) analysis indicated that formulations with lower concentrations of GA and MPI, and a minimal amount of CO (e.g., sample 1-541), exhibited the most stable color properties (average  $\Delta E = 1.38$ ), which is below 2. It may be due to the homogeneous membrane structures that reduce optical path interference and have high color uniformity. Conversely, formulations with excessive GA (e.g., 6%) or MP (4%) combined with higher oil content (2%), such as samples 1-342 and 1-642 showed  $\Delta E$  values exceeding 4. Excessive GA could lead to phase separation and form local aggregation areas.<sup>23</sup>

For the GE-based group, sample 2-442 showed the highest  $\Delta E$ , with the highest concentration of MPI. Microscopic observations revealed a relatively uniform distribution of oil droplets and a well-formed protein network (Fig. 1), suggesting effective

protein interactions and successful oil entrapment. However, elevated MPI concentrations may also promote protein aggregation, forming denser structures and increasing the refractive index contrast within the matrix. This phenomenon could enhance light scattering and reduce transmittance, ultimately resulting in lower brightness and decreased  $\Delta L^*$  values. Furthermore,  $\beta$ -aggregates induced by heat treatment at high MPI levels may lead to microphase separation during drying, causing localized thickness variations and surface irregularities, which visually manifest as darker and yellower films.<sup>19</sup> In contrast, sample 2-424 featured a lower MPI concentration and a relatively higher content of CO. Although its matrix was slightly less compact than that of 2-442, its overall structural balance indicated good emulsion stability. Studies have shown that lipid components can form smooth, continuous surfaces or finely dispersed aggregates within the film, enhancing specular reflection and reducing diffuse light scattering.<sup>24</sup> Additionally, due to their refractive index being closer to that of air, surface lipid layers or microvoids can facilitate better light transmission, thereby improving film brightness.<sup>25</sup> It is worth noting that although GE content varied among the samples, its influence on optical properties appeared minor compared to MPI and oils. GE primarily affects film-forming ability and mechanical characteristics, while its role in optical modulation is relatively limited.

### 3.3 Static contact angle measurement

The surface wettability of edible coatings is a key factor affecting their moisture and gas barrier performance. The water contact angle, as an important indicator characterizing hydrophilicity and hydrophobicity, not only determines the diffusion and adsorption behavior of water on the coating surface, but also largely affects the performance of the coating in food preservation.<sup>26</sup> The wetting behavior of the coating is closely related to its chemical composition (such as lipids, emulsifiers) and microstructure (such as surface uniformity and lipid distribution), and its sensitivity to water penetration is significantly higher than that to gas penetration. Especially in composite or emulsion film layer structures, whether the hydrophobic phase (such as lipids) in the coating is continuously and uniformly distributed is the key to determining its barrier performance.<sup>27</sup> The contact angles for all coatings are summarized in Fig. 3. All coatings showed contact angles smaller than 80°, indicating the relatively hydrophilic nature of the coatings, however, a more hydrophobic surface (higher contact angle) is desirable.

For the GA-based group, when measuring samples 1-642, 1-424, and 1-324, the shape of the water droplets changed immediately after contacting the coating, making it difficult to obtain the correct angles, indicating the relatively high hydrophobicity of these formulations. GA plays a role in the hydrophobicity of the coating, but the effect of GA alone on coating hydrophobicity, as 1-442 (67.7°) showed a larger contact angle than 1-342 (47.9°), when the GA content further increased (1-642, 34.9°), it became smaller again, while 1-424 (31.1°) showed a smaller contact angle than 1-324 (39.3°, Fig. 3). Additionally, the oil and MPI ratios also influenced the contact angles as their



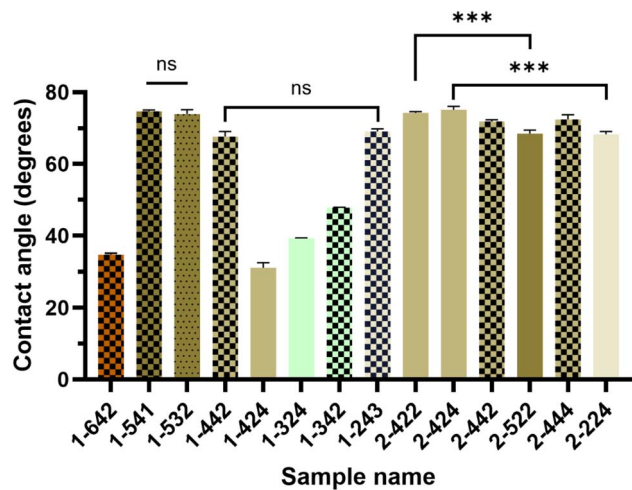


Fig. 3 Contact angles of all spray coating formulations, fill color darkness increases represents an increase of GA/GE concentrations, fill pattern density increases represents an increase of MPI concentration (\*\*\*)  $p < 0.001$ .

values changed from  $67.7^\circ$  (1-442) to only  $31.1^\circ$  (1-424), by simply swapping the MPI and oil ratio. Although there is no sample set which showed the effect of oil alone or MPI alone on the coating hydrophobicity while keeping the GA content consistent, it is notable that increasing MPI at the same oil level could reduce hydrophobicity, as MPI could provide emulsion stability. The hydrophobicity of the coating can be impacted by the emulsion structure driven by protein–protein interactions and their stabilizing effect on oil droplets. As reported in previous studies, although both polymers carry negative charges, partial charge neutralization can occur due to localized positive regions on the protein surface, especially at a pH of 6, leading to the formation of weak electrostatic complexes.<sup>23</sup> However, if the composition deviates from the optimal ratio (MPI:GA = 3:1) in an emulsion system (pH 5–7), these interactions may not be sufficient to produce a coherent, hydrophobic surface.<sup>28</sup> Consequently, the resulting film remains highly hydrophilic, with exposed polar groups allowing for rapid water uptake and preventing stable contact angle measurements.

For both the GA and GE-based groups, there was no clear trend that indicates the effect of oil content on film hydrophobicity, as the differences in contact angles were non-significant (Fig. 3). Collagen peptides are known for strongly adsorbing to surfaces, which makes them highly hydrophilic, therefore, it is interesting that this trend was not observed in this study. This might be due to the mechanism that GE is adsorbing on the surface of the glass slides due to its hydrophobic groups, while MPI stabilises oil droplets and preventing the oil to reach the surface of the coating, without reducing the contact angle by much.<sup>29</sup> Otherwise, the increase of the oil concentration would increase the coating contact angle. For example, Galus and Kadzińska reported that the incorporation of lipids significantly increased the contact angle and hydrophobicity of the whey protein-based films.<sup>30</sup> Mechanistically, this may be attributed to the migration and surface enrichment of CO during drying,

forming hydrophobic domains that increase surface free energy and inhibit water spreading.<sup>31</sup> Furthermore, at a higher oil content, the increase of GE showed a positive effect on coating hydrophobicity, as 2-424 had a significant larger contact angle than 2-224. However, when oil content is lower, the increase of GE concentration showed an opposite effect, as 2-522 had a significant smaller contact angle than 2-422. This result further supports the combined effect of GE and oil on the surface hydrophobicity of the coatings.

In addition to lipid content, the surface chemical composition and microstructure also influenced the contact angle of GE-based coatings. Films with rough surfaces (such as 2-442, 2-444, Fig. 2), dense and uniformly distributed oil droplets (such as 2-422, 2-444, and 2-424, Fig. 3) were more likely to expose hydrophobic domains, resulting in larger contact angles. This phenomenon can be explained by the Wenzel model, which suggests that surface roughness on hydrophilic substrates further decreases contact angle.<sup>32</sup>

Overall, the contact angles of GE-based group were generally higher than the GA-based group. Additionally, contact angles of films are not solely determined by the formulations, but are also governed by factors such as lipid migration, protein adsorption, structural compactness, and surface roughness. Optimizing the ratio of MPI, GE, and CO, along with controlling emulsion stability, is key to modulating surface hydrophobicity and improving water resistance in edible coatings.

### 3.4 Effect of coatings on bananas preservation

In order to evaluate the practical effect of these coatings on fruit preservation, bananas were selected as model samples in this study for a 10-day room-temperature storage experiment. Bananas were chosen as experimental samples for coating applications mainly because of their high perishability and extreme sensitivity to water loss and oxidation reactions. These characteristics make it highly suitable for evaluating the protective effects of edible coatings in extending shelf life, reducing moisture migration, and maintaining surface quality.<sup>33</sup> In addition, bananas undergo measurable changes during the processes of ripening and spoilage, such as browning, softening, water loss and skin collapse. It is convenient to record these changes by measuring their weight change, as well as through visual observation, which are suitable for verifying the protective effect of the coating. During the storage of fruit and vegetables, water evaporation is one of the main factors leading to weight loss and quality deterioration. Although the fruit peel has certain natural protective functions, it is still difficult to avoid the continuous loss of water through the pores or microcracks on the epidermis during storage. According to Nunes and Emond, even minor weight losses (3–10%) can lead to perceptible quality deterioration in fruit, including loss of firmness, shriveling, and color changes.<sup>34</sup>

Three groups were set up for both GA and GE-based samples: the blank control group without coating, and two (duplicated, noted as sample 1 and sample 2) experimental groups. By continuously recording the weight and visual appearance



changes of each sample, the preservation performance of the coating was further analyzed.

For GA-based group, within the first 3 days, the weight loss of coated samples was lower than that of the uncoated sample, indicating that the coating had an initial barrier effect on slowing down water evaporation. However, with the GA coating, it did not have a significant effect on weight loss reduction compared to the control group after day 7 (Fig. 4a). It is notable that sample 1 and sample 2 used the same coating formula (1-541), but in the later stage (after day 7), the weight loss curve of sample 2 was significantly greater and finally reached the maximum value (22.8%) on day 10, which was much higher than sample 1 and control group. According to the observation, there was a local damage phenomenon on the surface of sample 2, which is very likely caused during the previous operation or handling process. This damage greatly reduced the continuity and integrity of both the skin and the coating layer, allowing water to escape directly through the gap, accelerating water evaporation and weight loss compared to the control and coated samples. In contrast, the coating of sample 1 was intact. Its weight loss rate was relatively stable, verifying that this formula has a certain waterproof evaporation ability under the condition of intact epidermis. However, from day 3 onward, the weight loss curves of sample 1 and the control group exhibited a nearly overlapping trend, suggesting that the coating applied to sample 1 provided only limited efficacy in reducing moisture loss during the later stages of storage. Potential reasons may include insufficient coating thickness, poor film continuity, and the limited hydrophobicity of the GA/MPI/CO formulation at the applied concentration.

During the 10-day storage period at room temperature, all banana samples showed typical signs of post-ripening and aging, such as discoloration of the skin, softening of the visual

texture. However, it can be observed that there are significant differences in the rate and degree of deterioration between coated and uncoated samples (Fig. 4b), with a detailed comparative visual and textural evaluation (Table S4), and a deterioration scoring (Fig. S5). Sample 1 showed the slowest decline in sensory quality among the three groups. During the first 7 days, the fruit peel remained basically smooth, with only slight discoloration and signs of water loss. Even on day 10, only uniform browning occurred, and the fruit peel remained firm without collapsing. This indicates that the coating has played a good role in controlling water evaporation and oxidation reactions, which is in line with the mechanism for regulating the exchange of gas and water vapor. Although the formula used in sample 2 was the same as sample 1, due to the early damage of its skin, the continuity of the coating was impaired, thereby significantly weakening its preservation performance. After day 7, the deterioration of the sample accelerated significantly. Patchy black spots rapidly appeared on the epidermis, and it softened significantly. By day 9, the epidermis collapsed severely, the area of browning expanded, and rotting phenomena were observed in some areas. It can be inferred that the local damage has disrupted the original barrier, increased the permeability of water vapor and oxygen, and thereby induced accelerated breathing and tissue aging. This result highlights the decisive role of the structural integrity of the coating in its functional performance. The control group received no treatment and showed an obvious aging trend from the initial stage of storage. From day 3, color spots and softening appeared around the fruit stalks, and then the deterioration intensified rapidly. By day 10, the fruit peel turned black over a large area, the structure became loose, and the rotten juice oozed out, indicating that it had entered the stage of spoilage. Compared with the coating treatment group, the

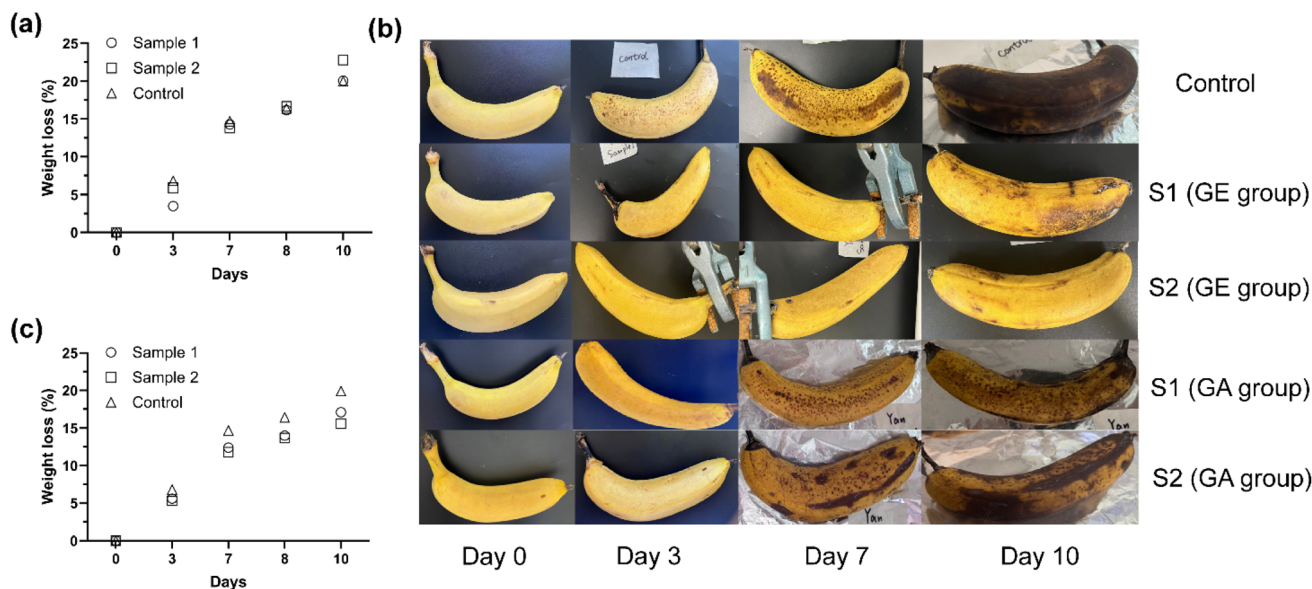


Fig. 4 Weight loss of GA sample 1-541 coated and uncoated (control) bananas (a), and representative images of banana samples including control group and two identical coated groups at day 0, day 3, day 7, and day 10, for both GE and GA group samples (b); weight loss of GE sample 2-424 coated and uncoated (control) bananas (c). Weight loss was reported as a weight percentage of sample's initial weight at day 0.



samples lacking surface barriers had the poorest storage stability, confirming the rapid aging characteristics caused by the high migration rates of water and oxygen in the untreated state.

For GE-based group, the weight loss of coated samples was lower than that of uncoated sample throughout the entire testing period (from day 0 to day 10, Fig. 4c), indicating the notable barrier effect of coating on maintaining moisture and preserving the bananas. The difference in weight loss was the most on day 10, as the control group lost 20% of its initial weight, while sample 2, particularly, only had a weight loss of 15.6%. The appearance of bananas with and without coating during the experimental periods indicated the same trend as the weight loss results, as both sample 1 and sample 2 showed a lower degree of post-ripening and aging, such as discoloration of the skin, softening of the texture and loosening of the structure compared to the control group, from day 0 to day 10 (Fig. 4b). On day 3, the coated samples largely retained their original color and firmness, with minimal browning observed. On day 7, the coated samples showed only limited brown spots, maintained a uniform yellow peel without large-scale discoloration, and remained relatively full and firm, while the control group showed more pronounced browning, with most of the peel appearing yellow-brown and marked with obvious brown speckles. Substantial moisture loss led to slight skin shriveling. On day 10, the control group developed extensive dark brown to black peel, suffered severe dehydration, and exhibited overly softened pulp with possible off-odors, rendering them largely inedible. In comparison, the coated bananas exhibited moderate browning and softening but retained parts of the yellow peel and relatively intact pulp structure, with minimal odor and reduced moisture loss.

These observations indicate that bananas coated with edible films experienced slower browning, reduced weight loss, and delayed texture deterioration during storage, demonstrating a notable preservation effect compared to the uncoated control group. The main mechanism underlying this effect is the edible coating's ability to regulate water evaporation, gas exchange, and ethylene production during storage.<sup>35</sup> Firstly, the coating serves as a barrier to water loss. By reducing transpiration at the fruit surface, the coating slows the rate of moisture loss during storage and helps maintain fruit freshness.<sup>36</sup> For example, bananas coated with chitosan-based edible films exhibited significantly lower weight loss than uncoated controls, confirming the coating's role in reducing water evaporation.<sup>37</sup> Moisture retention not only prevents premature peel shrinkage but also helps maintain pulp firmness and desirable texture.<sup>35</sup> Secondly, the semi-permeable barrier formed by edible coatings regulates gas exchange.<sup>37</sup> The coating reduces the influx of external oxygen and the efflux of internal carbon dioxide, thereby lowering the banana's respiration rate. Reduced respiration slows down metabolic activity, delaying nutrient depletion and energy release, which is crucial for suppressing postharvest ripening. Moreover, as a climacteric fruit, banana ripening and senescence are closely associated with rapid ethylene production. By limiting respiration and forming a gas barrier, the coating further inhibits ethylene synthesis and

accumulation.<sup>6</sup> Similar findings were reported by Yun *et al.*, where coating treatments significantly delayed banana ripening and quality degradation, consistent with the ethylene-suppressing mechanism.<sup>38</sup>

It is also notable that the GE-based coating (2-424) resulted in reduced banana weight loss and better maintenance of the fruit's original appearance and firmness compared to the GA-based coating (1-541). Both coatings exhibited similar hydrophobicity (contact angle  $\sim 75^\circ$ ) and comparable thickness ( $\sim 17 \mu\text{m}$ ). However, the GE-based coating 2-424 possessed a higher surface roughness ( $4.10 \mu\text{m}$  and  $2.98 \mu\text{m}$  of  $R_q$  and  $R_a$ , respectively) than GA-based coating 1-541 ( $3.29 \mu\text{m}$  and  $2.71 \mu\text{m}$  of  $R_q$  and  $R_a$ , respectively), which may have contributed to its superior preservation performance. Increased micro-roughness can enhance the apparent hydrophobicity by reducing the real contact area between water droplets and the surface, leading to more effective water repellence.<sup>39,40</sup> Moreover, a rougher microstructure can improve mechanical interlocking with the fruit peel, minimizing coating detachment and reducing microcrack formation during storage, thereby limiting moisture and gas exchange.<sup>41</sup> These factors collectively suggest that the enhanced surface structuring of the GE-based coating may have provided a more robust barrier against degradation processes in bananas. In summary, edible coatings reduce water loss and gas exchange, resulting in decreased respiration and ethylene generation in bananas. These effects collectively slow post-ripening changes such as browning and softening, significantly extending shelf life and maintaining edibility.

### 3.5 Discussion on limitations and future perspectives

This study has demonstrated the potential of GE- and GA-based edible coatings to reduce water loss and delay ripening in bananas. Nonetheless, several limitations deserve discussion in the context of prior literature, and future research directions can build upon both our strengths and the gaps identified.

**3.5.1 Formulation-related considerations.** Although this study focused on single-component GE and GA coatings, prior research on protein-polysaccharide composites suggests that blending these polymers can yield films with improved mechanical and barrier properties. For example, Yoo and Krochta reported that whey protein isolate (WPI) blended with polysaccharides (methylcellulose, HPMC, sodium alginate) resulted in films with intermediate oxygen permeability and tensile strength compared to pure components.<sup>42</sup> Similarly, WPI blended with psyllium seed gum exhibited higher elongation at break and reduced oxygen permeability than the individual components.<sup>43</sup> These studies indicate that a GE + GA blend could enhance flexibility, strength, and preservation efficacy, while our single-polymer formulations provide a critical baseline for future optimization.

Furthermore, the use of animal-derived polymers such as GE and milk protein may restrict applicability for vegan or vegetarian consumers. Future research could explore plant-based alternatives or test these coatings on food matrices where animal-derived ingredients are acceptable, such as dairy or meat products.



**3.5.2 Methodological limitations and future improvements.** Spray-coating was chosen in this study for its laboratory convenience and reproducibility, but scalability to industrial applications remains a challenge. Other techniques, such as immersion or dipping, may be more practical for large-scale production.<sup>41</sup> Future work should directly compare the performance and uniformity of spray vs. dipping for GE/GA coatings, to evaluate feasibility under commercial conditions.

Another limitation concerns contact angle measurements, which were conducted on flat glass slides due to the curvature and heterogeneity of banana peel surfaces. The real fruit surface, with its natural wax layer and microstructure, may exhibit differences in coating adhesion and uniformity. Similar issues have been reported in other coating studies,<sup>32</sup> and future work should include direct measurements on the fruit surface to better assess practical coating performance.

**3.5.3 Characterization and data limitations.** Our study mainly focused on surface and optical properties (e.g., morphology and transparency), while mechanical properties such as tensile strength, flexibility, and hardness were not measured due to equipment constraints. Mechanical integrity is crucial for barrier function and durability; other studies have highlighted the importance of these measurements to correlate coating performance with postharvest quality.<sup>44</sup>

Additionally, peel color was assessed visually, and only one banana per treatment was evaluated for sensory analysis. These factors limit statistical robustness and reproducibility. Standard postharvest studies often employ larger sample sizes, instrumental color and texture analyses, and expanded sensory panels for more reliable conclusions. Future work should adopt these approaches, including evaluation of taste and mouthfeel, to more comprehensively assess coating acceptability.

**3.5.4 Scope expansion and integration with other preservation technologies.** Bananas were used as a model fruit, but results may not generalize to fruits with different skin structures or higher moisture content, such as grapes or strawberries. Testing a broader range of fruit types will provide insights into the versatility and limitations of GE and GA coatings.

Moreover, this study did not combine the coatings with other postharvest preservation strategies, such as Modified Atmosphere Packaging (MAP). Prior research has shown that coating + MAP can offer synergistic benefits, including reduced respiration, delayed microbial growth, and maintained visual quality.<sup>45</sup> By isolating the coating effect, our study establishes a baseline, which can serve as a reference for future research exploring integrated preservation approaches for enhanced shelf life and sustainability.

## 4 Conclusions

This study successfully developed a transparent, water-resistant, and edible spray coating system formulated from natural biopolymers, including GE, GA, MPI, and CO, addressing the dual challenges of post-harvest preservation and environmental sustainability. By systematically optimizing formulation ratios and spraying parameters, fourteen GA- and

GE-based coatings with varying biopolymer-to-oil ratios were prepared and evaluated. Coating performance was comprehensively characterized across multiple dimensions, including optical transmittance, water contact angle, surface morphology, thickness and roughness, color stability, viscosity, and microstructure, revealing relationships between structural features and functional properties. Among all formulations, sample 1-541 (5% GA, 4% MPI, 1% CO) from the GA-based group and sample 2-424 (4% GE, 2% MPI, 4% CO) from the GE-based group exhibited the most balanced performance, combining structural integrity, hydrophobicity, visual transparency, and mechanical stability. Optical microscopy confirmed dense, smooth, crack-free films with high uniformity. Banana preservation trials demonstrated that the GE based coating effectively reduced water loss up to 10 days. Based on visual assessment of ripening color and odor, both the GA and GE coatings delayed ripening, and maintained quality during storage. Overall, this work presents a novel edible spray coating system with strong potential for sustainable packaging and large-scale post-harvest treatment, offering a promising pathway toward reducing food waste while minimizing environmental impact.

Future research should focus on advancing GA/GE-based coatings from passive moisture barriers to active preservation systems by incorporating natural antimicrobial, antioxidant, and antifungal compounds to suppress spoilage and extend the shelf life of fresh produce. Long term storage trials spanning several weeks to months are necessary to evaluate the retention of barrier properties, mechanical integrity, antimicrobial efficacy, and the effects on sensory attributes such as appearance, firmness, flavor, and texture. Furthermore, the application of advanced analytical techniques, such as Fourier Transform Infrared Spectroscopy (FTIR), pendant drop evaluation of interfacial properties, surface evaluation using quartz crystal microbalance with dissipation, texture evaluation by dynamic mechanical analysis and structural evaluation by scanning electron microscopy (SEM), will enable detailed characterization of molecular interactions, structural features, and microstructural changes during storage. Such multidimensional investigations will provide a deeper understanding of the relationships between formulation, structure, and preservation performance, ultimately guiding the development of more effective edible coatings. Several limitations remain in the work. The number of formulations can be expanded in future tests to further enhance water repellency. Testing the coatings on different fruits would also strengthen the evidence of their applicability. Additionally, the influence of spraying speed and angle should be investigated in more detail to optimize coating performance.

## Conflicts of interest

There are no conflicts to declare.

## Data availability

The data supporting the findings of this study are available from the corresponding author upon reasonable request.



Supplementary information (SI) is available. See DOI: <https://doi.org/10.1039/d5fb00804b>.

## Acknowledgements

We acknowledge the support provided by the Australian Government Department of Education and the University of Queensland through Australia's Food and Beverage Accelerator (FaBA). We acknowledge Dr Joseph Nastasi from the University of Queensland for the spray gun. We acknowledge GELITA Australia Pty. Ltd For the GE material.

## References

- 1 A. Sridhar, M. Ponnuchamy, P. S. Kumar and A. Kapoor, Food preservation techniques and nanotechnology for increased shelf life of fruits, vegetables, beverages and spices: a review, *Environ. Chem. Lett.*, 2021, **19**(2), 1715–1735.
- 2 S. Shankar, A. K. Mohanty, J. R. DeEll, K. Carter, R. Lenz and M. Misra, Advances in antimicrobial techniques to reduce postharvest loss of fresh fruit by microbial reduction, *npj Sustain. Agric.*, 2024, **2**(1), 25.
- 3 A. M. C. N. Rocha, E. C. Coulon and A. M. M. B. Morais, Effects of vacuum packaging on the physical quality of minimally processed potatoes, *Food Serv. Technol.*, 2003, **3**(2), 81–88.
- 4 M. J. Gidado, A. A. N. Gunny, S. C. B. Gopinath, A. Ali, C. Wongs-Aree and N. H. M. Salleh, Challenges of postharvest water loss in fruits: Mechanisms, influencing factors, and effective control strategies – A comprehensive review, *J. Agric. Food Res.*, 2024, **17**, 101249.
- 5 P. G. C. Nayanathara Thathsarani Pilapitiya and A. S. Ratnayake, The world of plastic waste: A review, *Cleaner Mater.*, 2024, **11**, 100220.
- 6 M. Shams, I. Alam and M. S. Mahbub, Plastic pollution during COVID-19: Plastic waste directives and its long-term impact on the environment, *Environ. Adv.*, 2021, **5**, 100119.
- 7 K. J. Groh, T. Backhaus, B. Carney-Almroth, B. Geueke, P. A. Inostroza, A. Lennquist, *et al.*, Overview of known plastic packaging-associated chemicals and their hazards, *Sci. Total Environ.*, 2019, **651**(Pt 2), 3253–3268.
- 8 Y. Zhang, S. Zhang and S. Wu, Room-temperature fabrication of TiO<sub>2</sub>-PHEA nanocomposite coating with high transmittance and durable superhydrophilicity, *Chem. Eng. J.*, 2019, **371**, 609–617.
- 9 F. Xiang, Y. Xia, Y. Wang, Y. Wang, K. Wu and X. Ni, Preparation of konjac glucomannan based films reinforced with nanoparticles and its effect on cherry tomatoes preservation, *Food Packag. Shelf Life*, 2021, **29**, 100701.
- 10 P. Criado, C. Fraschini, D. Becher, F. G. Mendonça Pereira, S. Salmieri and M. Lacroix, Modified cellulose nanocrystals (CNCs) loaded in gellan gum matrix enhance the preservation of *Agaricus bisporus* mushrooms, *J. Food Process. Preserv.*, 2020, **44**(11), e14846.
- 11 J. Jeya Jeevahan, M. Chandrasekaran, S. P. Venkatesan, V. Sriram, G. Britto Joseph, G. Mageshwaran, *et al.*, Scaling up difficulties and commercial aspects of edible films for food packaging: A review, *Trends Food Sci. Technol.*, 2020, **100**, 210–222.
- 12 T. Suzuki, C. Ito, K. Kitano and T. Yamaguchi, CIELAB Color Space as a Field for Tracking Color-Changing Chemical Reactions of Polymeric pH Indicators, *ACS Omega*, 2024, **9**(34), 36682–36689.
- 13 J. Ren, Y. Sun, J. Hui, R. Ahmad and Y. Ma, Coating thickness optimization for a robotized thermal spray system, *Robot. Comput. Integrated Manuf.*, 2023, **83**, 102569.
- 14 K. Dangaran, P. M. Tomasula and P. Qi, Structure and function of protein-based edible films and coatings, *Edible Films and Coatings for Food Applications*, Springer, 2009, pp. 25–56.
- 15 P. Doruker and W. L. Mattice, Effect of Surface Roughness on Structure and Dynamics in Thin Films, *Macromol. Theory Simul.*, 2001, **10**(4), 363–367.
- 16 A. Larena, F. Millán, G. Pérez and G. Pinto, Effect of surface roughness on the optical properties of multilayer polymer films, *Appl. Surf. Sci.*, 2002, **187**(3), 339–346.
- 17 L. Cwiklik, Tear film lipid layer: A molecular level view, *Biochim. Biophys. Acta Biomembr.*, 2016, **1858**(10), 2421–2430.
- 18 T. M. Ho, A. Razzaghi, A. Ramachandran and K. S. Mikkonen, Emulsion characterization via microfluidic devices: A review on interfacial tension and stability to coalescence, *Adv. Colloid Interface Sci.*, 2022, **299**, 102541.
- 19 D. H. U. Eranda, M. Chaijan, W. Panpipat, S. Karnjanapratum, M. A. Cerqueira and R. Castro-Muñoz, Gelatin-chitosan interactions in edible films and coatings doped with plant extracts for biopreservation of fresh tuna fish products: A review, *Int. J. Biol. Macromol.*, 2024, **280**, 135661.
- 20 F. Weinbreck, R. H. Tromp and C. G. de Kruif, Composition and Structure of Whey Protein/Gum Arabic Coacervates, *Biomacromolecules*, 2004, **5**(4), 1437–1445.
- 21 K. Kaur, N. Gupta, M. Mahajan, S. K. Jawandha and N. Kaur, A novel edible coating of beeswax impregnated with karonda polyphenol rich extract maintains the chemical and bioactive potential of fresh ber fruit during storage at low temperature, *Hortic., Environ. Biotechnol.*, 2023, **64**(6), 1001–1014.
- 22 Q. O. Tiamiyu, S. E. Adebayo and A. A. Yusuf, Gum Arabic edible coating and its application in preservation of fresh fruits and vegetables: A review, *Food Chem. Adv.*, 2023, **2**, 100251.
- 23 M. Erben, A. A. Pérez, C. A. Osella, V. A. Alvarez and L. G. Santiago, Impact of gum arabic and sodium alginate and their interactions with whey protein aggregates on bio-based films characteristics, *Int. J. Biol. Macromol.*, 2019, **125**, 999–1007.
- 24 W. K. Subczynski, M. Pasenkiewicz-Gierula, J. Widomska, L. Mainali and M. Raguz, High Cholesterol/Low Cholesterol: Effects in Biological Membranes: A Review, *Cell Biochem. Biophys.*, 2017, **75**(3–4), 369–385.
- 25 A. Jiménez, M. J. Fabra, P. Talens and A. Chiralt, Effect of lipid self-association on the microstructure and physical properties of hydroxypropyl-methylcellulose edible films



- containing fatty acids, *Carbohydr. Polym.*, 2010, **82**(3), 585–593.
- 26 V. Morillon, F. Debeaufort, G. Blond, M. Capelle and A. Voilley, Factors Affecting the Moisture Permeability of Lipid-Based Edible Films: A Review, *Crit. Rev. Food Sci. Nutr.*, 2002, **42**(1), 67–89.
- 27 L. S. Devi, A. K. Jaiswal and S. Jaiswal, Lipid incorporated biopolymer based edible films and coatings in food packaging: A review, *Curr. Res. Food Sci.*, 2024, **8**, 100720.
- 28 M. Klein, A. Aserin, P. B. Ishai and N. Garti, Interactions between whey protein isolate and gum Arabic, *Colloids Surf., B*, 2010, **79**(2), 377–383.
- 29 H. M. Shewan, M. Siauw, N. Vinden, A. Dong, A. Beheshti, K. Y. Chew, J. R. Stokes, K. R. Short, D. Mikkelsen, B. Koehler and M. Reihmann, Developing an antiviral surface cleaner utilising unique surface adsorption properties of hydroxyproline-rich-proteins, *Household Pers. Care Today*, 2022, **17**(5), 57–61.
- 30 S. Galus and J. Kadzińska, Moisture Sensitivity, Optical, Mechanical and Structural Properties of Whey Protein-Based Edible Films Incorporated with Rapeseed Oil, *Food Technol. Biotechnol.*, 2016, **54**(1), 78–89.
- 31 X. Yu, L. Chen, Z. Jin and A. Jiao, Research progress of starch-based biodegradable materials: a review, *J. Mater. Sci.*, 2021, **56**(19), 11187–11208.
- 32 S. Krainer and U. Hirn, Contact angle measurement on porous substrates: Effect of liquid absorption and drop size, *Colloids Surf., A*, 2021, **619**, 126503.
- 33 P. Deng, Y. Zhang, Q. Deng, Y. Sun, Y. Li, Z. Wang, *et al.*, Multifunctional sodium alginate-based self-healing edible cross-linked coating for banana preservation, *Food Hydrocolloids*, 2024, **151**, 109753.
- 34 C. Nunes and J. Emond, Relationship between weight loss and visual quality of fruits and vegetables, *Proceedings of the Florida State Horticultural Society*, Goldenrod Florida State Horticultural Society, Palm Beach County, Florida, USA, 2007, pp. 235–245, pan: 20183290851.
- 35 R. Santhosh, J. Ahmed, R. Thakur and P. Sarkar, Starch-based edible packaging: rheological, thermal, mechanical, microstructural, and barrier properties - a review, *Sustainable Food Technol.*, 2024, **2**(2), 37–3.
- 36 F. M. Dwivany, A. N. Aprilyandi, V. Suendo and N. Sukriandi, Carrageenan Edible Coating Application Prolongs Cavendish Banana Shelf Life, *Int. J. Food Sci.*, 2020, **2020**(1), 8861610.
- 37 K. Priya, N. Thirunavookarasu and D. V. Chidanand, Recent advances in edible coating of food products and its legislations: A review, *J. Agric. Food Res.*, 2023, **12**, 100623.
- 38 Z. Yun, H. Gao, X. Chen, X. Duan and Y. Jiang, The role of hydrogen water in delaying ripening of banana fruit during postharvest storage, *Food Chem.*, 2022, **373**, 131590.
- 39 M. Mu, W. Zhou, Y. Arcot, L. Cisneros-Zevallos and M. Akbulut, Edible superhydrophobic coating derived from triterpenoid maslinic acid for bacterial antifouling and enhanced fresh produce food safety, *Food Packag. Shelf Life*, 2024, **43**, 101290.
- 40 M. J. Gidado, A. A. N. Gunny, S. C. B. Gopinath, M. Devi, R. Jayavalli and R. A. Ilyas, Challenges in selecting edible coating materials for fruit postharvest preservation and recent advances in edible coating techniques: a review, *J. Food Sci. Technol.*, 2025, **62**(4), 612–622.
- 41 A. Monasterio, E. Núñez, N. Brossard, R. Vega and F. A. Osorio, Mechanical and Surface Properties of Edible Coatings Elaborated with Nanoliposomes Encapsulating Grape Seed Tannins and Polysaccharides, *Polymers*, 2023, **15**(18), 3774.
- 42 S. Yoo and J. M. Krochta, Whey protein-polysaccharide blended edible film formation and barrier, tensile, thermal and transparency properties, *J. Sci. Food Agric.*, 2011, **91**(14), 2628–2636.
- 43 X. Zhang, Y. Zhao, Y. Li, L. Zhu, Z. Fang and Q. Shi, Physicochemical, mechanical and structural properties of composite edible films based on whey protein isolate/psyllium seed gum, *Int. J. Biol. Macromol.*, 2020, **153**, 892–901.
- 44 S. S. N. Chakravartula, M. Soccio, N. Lotti, F. Balestra, M. Dalla Rosa and V. Siracusa, Characterization of Composite Edible Films Based on Pectin/Alginate/Whey Protein Concentrate, *Materials*, 2019, **12**(15), 2454.
- 45 X. Liao, Y. Xing, X. Fan, Y. Qiu, Q. Xu and X. Liu, Effect of Composite Edible Coatings Combined with Modified Atmosphere Packaging on the Storage Quality and Microbiological Properties of Fresh-Cut Pineapple, *Foods*, 2023, **12**(6), 1344.

